

Real-time, Cuff-less and Non-invasive Blood Pressure Monitoring

Alireza Abolhasani, Morteza Mousazadeh, Abdollah Khoei

Urmia University, Microelectronic Research Laboratory, Urmia, Iran

Abstract: In this study ultrasonic method was applied for the measurement of blood pressure (BP). First, a novel method is proposed to measure mean arterial pressure (MAP), diastolic blood pressure (DBP) and systolic blood pressure (SBP) using ultrasonic sensors. The proposed algorithm is implemented by measuring the diameter of the artery and the speed of blood flow based on Doppler physical phenomena so that the BP can be calculated. The results of the proposed algorithm for MAP, SBP, and DBP hypertension analyses were evaluated with the results of Association for the Advancement of Medical Instrumentation (AAMI standard) for all three cases and their mean error rate for the worst case was -0.233mmHg and the standard deviation for 422 samples taken from individuals in the worst case was 4.53 mmHg that meets the standard requirements. Also, according to the British Hypertension Society (BHS) standard, the proposed algorithm for the estimation of BP for all three cases of MAP, DBP, and SBP has Grade A, indicating its higher accuracy in measuring and using the most effective variables in the diagnosis of hypertension in the human body. The proposed algorithm in BP estimation is non-invasive, cuff-less which needs no calibration, and is only based on using the ultrasonic sensor.

Keywords: cuff-less; continues monitoring; blood pressure

Neinvazivno merjenje krvnega tlaka v realnem času brez uporabe manšete

Izveček: V članku je predstavljena metoda meritve krvnega tlaka z ultrazvočnimi senzorji. Najprej je predstavljena nova metoda merjenja povprečnega (MAP), diastoličnega (DBP) in sistoličnega tlaka (SBP) z uporabo ultrazvočnih senzorjev. Predlagan algoritem temelji na meritvi preseka žile in hitrosti pretoka krvi na osnovi dopplerjevega pojava. Rezultati meritev so preverjeni z rezultati meritev po AAMI standardu. Povprečna napaka vseh treh veličin na najslabšem primeru je bila -0.233 mmHg s standardno napako 5.53 mmHg . Glede na britansko združenje BHS se metoda uvršča v razred A meritev krvnega tlaka. Metoda je neinvazivna brez uporabe manšete

Ključne besede: brez manšete; nepretrgane meritve; krvni tlak

* Corresponding Author's e-mail: m.mousazadeh@urmia.ac.ir

1 Introduction

Cardiovascular disease (CVD) is one of the main causes of death in the world. According to the European Heart Institute reports, 4.1 million people die from the disease each year [1]. Long-term hypertension is one of the most important risk factors for coronary artery disease, stroke, heart failure, atrial fibrillation, peripheral vascular disease, vision loss, chronic kidney disease and dementia [15-17]. The prevalence of hypertension in 2014 was 1.3 billion worldwide, and it is projected to reach 1.56 billion by 2030 [2, 3].

Blood pressure (BP) is one of the most important parameters of the human body where by its measure-

ment, very useful information can be provided for the physician. Repeated measurements of BP can lead to early diagnosis of the disease, which can be controlled and treated owing to the early diagnosis [4]. By definition, BP is the pressure exerted by blood on the walls of a blood vessel. Its value depends on the functional factors of the cardiovascular system, such as the strength of the cardiac extrusion, the flexibility, and the thickness of the vessel wall [5]. This pressure applied to the vessel wall differs in the two modes of cardiac function and resting phase, which are termed the systolic pressure-maximum pressure (SBP) and the diastolic pressure-minimum pressure (DBP) respectively [6].

According to the National Heart, Lung and Blood Institute (NHLBI), standard systolic and diastolic BP values are 120 and 80 mmHg, respectively. So, BP can be considered in a range which varies proportional to each heartbeat [7]. Another important factor in BP measurement is obtaining the mean blood pressure (MAP) that can be calculated using equation (1).

$$\text{MAP} = (2\text{DBP} + \text{SBP})/3 \quad (1)$$

In health centers, BP is generally measured with a cuff, which is the most common method for its estimation [8]. Although the measurement of BP using cuff-based methods is meticulously acceptable and reliable, this method is completely dependent on the ability of the one who performs the measurement. Furthermore, cuff-based methods cannot be directly and continuously used because they require several minutes of interruption between each measurement [18]. Hence, the challenges of measurement using the cuff are: BP measurement during movement, the harmfulness of this type of pressure measurement for the patient's cardiovascular system, the inability of the device in continuous measurement, The cuff weight itself, patients' dissatisfaction with the use of cuffs under specific conditions, such as exercise testing and Ambulatory Blood Pressure Monitoring (ABPM) [5, 9, 10]. In the last two decades, there have been extensive studies over non-invasive BP measurement without applying cuff that has led to good results. Amongst these technologies are wearable sensors used by typical people daily, such as smart watches, which provide useful information about vital signs of the body. Many sensors that are used to gather vital body information such as body temperature, heart rate, the amount of oxygen for blood saturation and blood sugar, etc. can be made of flexible and portable materials so that they are easy to use [24 to 29]. This article aims at presenting a novel method for measuring BP in a non-invasive way without using cuff. In order to measure BP without using cuff, some other methods have been proposed, in which most of the mathematical relationships and estimation of BP are obtained from one of the measured elements of the body by either using sensors or by imaging the desired vessel as well as extracting their features using image processing techniques [72].

One of the most commonly used non-invasive BP measurements is Pulse Transit Time (PTT) [11]. The pulse transit time is when the heartbeat reaches the desired sensor mounted on the body. In many cases, researchers use electrocardiographic (ECG) signals and sensors (PPGs) to measure BP using this method. PTT measurements can be implemented by one ECG sensor and one PPG sensor or two PPG sensors [12]. The proper reception of the ECG signal requires at least three electrodes at three different points of the body.

Patient movement, poor electrode contact with the skin surface and electrode wires for prolonged reception can cause signal noise, which is a limiting factor for measuring BP based on this method [9, 13]. The high cost of using these different devices and sensors, the difficulties associated with installing sensors in different parts of the body and their interconnection with the central control system is a great concern in using this method to measure BP. As has been frequently reported, using PTT due to the dynamic nature of human muscles and hydrostatic changes cannot be a reliable method for measuring BP [20]. A simple and efficient way to directly measure BP using PPG sensors has been reported. In which they used a kind of regression modeling between the amplitude of the signals obtained from PPG sensors to estimate BP [21]. The results of this method were promising for estimating systolic BP, but in the estimation of diastolic pressure did not have a good performance and had significant errors. Furthermore, since regression has no memory, it cannot model the delay between the received PPG signal and the instantaneous BP which in turn, it can create some errors in the measurement [22]. Although this method is perfectly suited for modeling the portable systems, it has complex computations. In addition, the BP and the results of PPG sensors are not constant due to dynamic human muscle changes and hydrostatic vascular changes, so the application of this method may be limited to certain conditions. Particularly, if somebody would like to estimate BP using PPG, considering the fact that this method is based on measuring the amount of oxygen in the blood and when there are disorders such as hypoxia (hypoxia), this method cannot be practically used [23]. In [31] a new method has been reported for extracting BP characteristics from the amplitude and frequency of the signal received from the body based on PTT and Fourier Series Transform (FFT). In all the studies based on the extraction of amplitude and frequency information, after the formation of the characteristic vector and system training steps, using different machine learning algorithms such as regression algorithms, neural network [33] and fuzzy logic [10] The BP estimation is possible. These methods, in which the features are extracted in the form of a signal, are called the parameter-based approach. This method has a lot of complexities and errors, so it is desirable to use more accurate methods to obtain BP. All the above-mentioned methods estimate BP somehow by measuring one of the characteristics of the body's blood transfusion system and generalizing it to different conditions.

It must be mentioned that the Bernoulli method can also be of interest for BP measurement. However, if we want to employ such a method, we need to measure the primary pressure. Therefore, it is not applicable for our purpose.

According to the points mentioned above, in all these methods the amount of BP is measured indirectly by measuring one of the effects of increasing or decreasing BP in different parts of the body. On the contrary to what has been said earlier, the method presented in this paper, for the first time, directly examines the effect of blood changes on the blood vessels to measure BP very accurately. In the proposed method, the ultrasonic sensor is used to measure the transmitted and received waves, and after receiving the information from the ultrasonic sensor, using the Doppler physical phenomenon the vessel diameter and blood velocity are obtained, and then using the presented equations the amount of BP is calculated. Due to the flexibility and elasticity of the blood vessels, as the blood passes through them, the diameter of the vessels and then the volume of blood passing through the artery varies fully depending on the BP [14]. If the blood volume changes are accurately measured, they will have a waveform similar to Figure 1 and their frequency will be the same as the heart's operating frequency [30]. The above signal can be divided into two parts. The upper part of the signal is related to the heart or systole, while the lower part is attributed to the diastole.

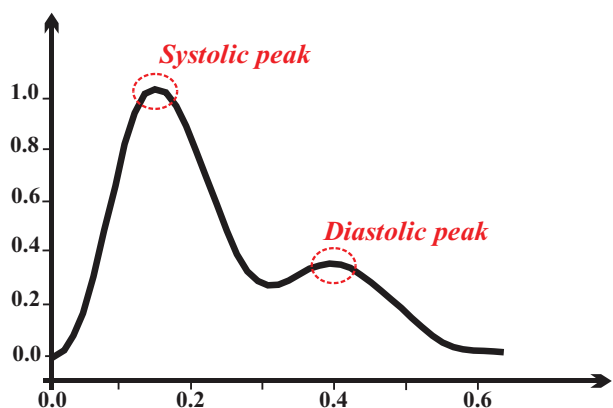


Figure 1: The volume of blood vessels in one cardiac cycle

2 Hypothesis and objectives

The main idea behind the paper was to introduce a continuous-time, cuff-less method for the measurement of the BP. According to the provided expressions in this study, the main parameters such as error, blood density and the diameter of the artery are supposed to have constant values.

3 Materials and methods

How to describe and measure the elastic behavior of the arteries is of a great importance, since from the as-

pect of basic physiology in the clinical domain, the risk of cardiovascular disease has been more prevailing. In 1960, Patterson is. [34]

$$E_p = \frac{\Delta P}{(\Delta D / D)} \tag{2}$$

In Patterson equation (E_p), P and D represent the pressure and the diameter respectively. The reverse of equation 2 was introduced in 1975 as the “arterial compliance” [2].

$$C = (\Delta D / D) / \Delta P \tag{3}$$

Since then, however, various authors have used the term “distensibility” for such cases which led to a greater association between mechanics and medical science. Accordingly, the authors recommend that this difference in terms all referring to the inverse of the elastic modulus be disregarded. Instead, they had better use some terms which are well-defined and appropriately used in various disciplines and replace “elastic modulus” and “compressibility” with “compliance” and “distensibility” [36-38].

In classical physics, the “elasticity” is measured by increasing the force, the amount of deformation of the isotropic sample, and finally, using these values the stress-strain curve is obtained. The amount of deformation of a specimen will depend on the elastic modulus and its geometry (length and cross-section). In engineering designs, the information about the behavioral properties of materials is required, regardless of their geometry. Thus, to eliminate the effect of geometry, the existing data is converted to other parameters. For this purpose, the amount of tensile or applied compressive force and the deformation values are converted to stress and strain respectively. The relationship between stress and strain is linear until the material reaches the Yield strength. E_p represents the slope of this part of

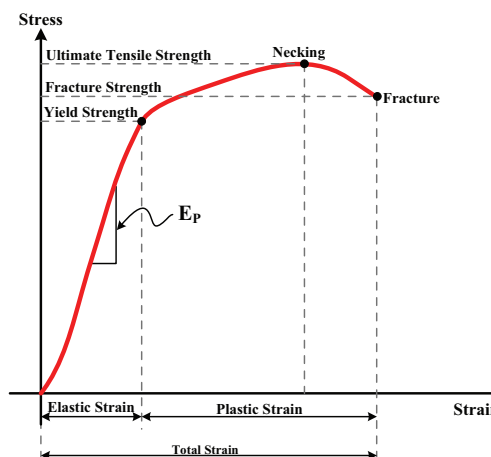


Figure 2: Stress-strain diagram

the curve which is identified by Young's modulus or the modulus of elasticity that can be used to calculate E_p of material by Hook's law as shown in Figure 2.

ΔV_{volume} the change in volume V_{volume} from the isotropic material that is created in response to the pressure change ΔP , the value of $V_{\text{volume}} \times \Delta P / \Delta V_{\text{volume}}$ is known as the "volume elasticity coefficient" and is usually denoted by the letter K.

In [39-40], in expression was driven for the forward going velocity of the pressure pulse, ΔP , in an infinitely long, thin-walled elastic tube filled with an essentially incompressible fluid and with the elasticity of the tube wall was considered to be isotropic. This has been known as the characteristic pulse wave velocity as shown in the equation below if we consider blood as the expected fluid and the artery equivalent to a very long tube with thin walls;

$$PWV_c = \sqrt{K/\rho} \tag{4}$$

In this equation, ρ is the density of blood and K is the elastic modulus of luminal volume change, per unit length of the artery (artery containing refined blood), which is calculated from equation 5.[78]

$$K = V_{\text{Volume}} \times \frac{\Delta P}{\Delta V_{\text{Volume}}} \tag{5}$$

It may be noted that since $V_{\text{Volume}} = \frac{4}{3} \pi R^3$ where R is the luminal radius and, and $dV_{\text{Volume}} = 4\pi R^2 \times dR$ if we consider ΔV_{Volume} to be small enough

$\frac{dV_{\text{Volume}}}{V_{\text{Volume}}} = \frac{\Delta V_{\text{Volume}}}{V_{\text{Volume}}} = 3 \times \frac{\Delta R}{R} = 3 \times \frac{\Delta D}{D}$ then equation 2 can be written as following.

$$K = \frac{\Delta P}{3 \times \frac{\Delta D}{D}} = \frac{\Delta P}{\frac{\Delta V_{\text{Volume}}}{V_{\text{Volume}}}} \tag{6}$$

Using Young-Laplace Equation Theory of Young-Laplace Equation and for thin-walled tubes, it can be concluded that the stress of the T-ring on the arterial wall with thickness t and radius R depends on the luminal pressure P and is obtained using the following equation [40].

$$T = P \times R/t \tag{7}$$

If we rewrite this equation based on the pressure, then the Barlow's Formula will be obtained.

$$P = T \times t/R \tag{8}$$

If the pressure P changes with a little value change as ΔP , then the stress will change with the little change value of ΔT using the following equation.

$$\Delta T = \Delta P \times R/t \tag{9}$$

Therefore, E_{inc} can be defined for static incremental Young's modulus for arterial wall type:

$$E_{\text{inc}} \equiv \text{stress/strain} = \left[\frac{\Delta P \times R}{t} \right] / \left[\frac{\Delta R}{R} \right] \tag{10}$$

$$E_{\text{inc}} = \Delta P \times D^2 / 2t \times \Delta D = \frac{K \times D}{2 \times t} \tag{11}$$

Since then the relation of pulse wave velocity can be written as follows:

$$PWV = \sqrt{E_{\text{inc}} \times t / 3 \times R \times \rho} \tag{12}$$

Relation 12 refers to the Moens-Korteweg equation [41-42]. This equation assumes that the arterial wall is isotropic and experiences isometrics changes with the pulse pressure.

A detailed study of the structure of the arterial wall reveals that the three main components of arterial wall elasticity are: collagen, elastin, and smooth muscle, which cause different K values.[43-46] Thus, the value of K for each artery will vary with the pressure and the amount of stress applied [47-49]. As a result, a constant K value cannot be used in the analyses and accordingly in the estimation of BP because the K value is directly related to the individual, the material of vessels and many other factors that are unique to each individual.

Therefore, it is proposed to describe the tensile behavior of the arterial walls, namely the elastic modulus for the volume change per unit length of the lumen and its inverse, that is, the amount of compression.

4 The proposed method

According to the explanations given in the previous sections, and knowing the pulse velocity equation, we can rewrite equation 12 as equation 13.[79-80]

$$V_{\text{Velocity}} = \sqrt{\frac{tE}{\rho d}} \tag{13}$$

In this equation, V_{velocity} is the velocity of blood passing through the vessel and t is the thickness of the artery, E

is the Young's module, d is the diameter of the vessel, ρ is the density of blood, and in this regard, the value of E can be substituted by 14, where E_0 is the value of the Young's module at the pressure of zero and it is always about 33.7 to 63.7mmhg and also the coefficient α of the arteries that is always in the range 0.016 to 0.018 mmhg-1.[74-75]

$$E = E_0 e^{\alpha p} \tag{14}$$

Substituting the relation 15 [76-77] into relation 14, will have:

$$V_{Velocity} = \sqrt{\frac{t \cdot E_0 \cdot e^{\alpha p}}{\rho \cdot d}} \tag{15}$$

Then, after several steps of simplification and obtaining the parameter p from the relation 15, we will have:

$$P = \frac{1}{\alpha} \ln \left(\frac{\rho d V_{Velocity}^2}{t E_0} \right) \tag{16}$$

The relation 16 is presented as the final relation for measuring the BP in which ρ is the density of blood with a value of 1080 kg/m³ and t is the approximate thickness of the vessels which is 0.46mm.

If we obtain the values of $V_{Velocity}$ for the velocity of blood flow through the artery and also the value of d for the diameter of the arterial vessels, we will be able to find the BP. The description given is shown as below:

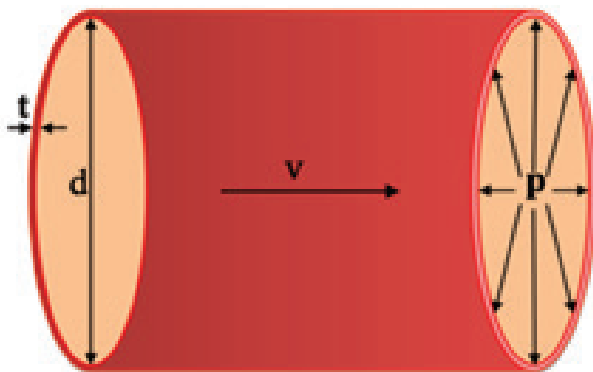


Figure 3: Artery and its related parameters

Therefore, in order to obtain BP, we need to find the diameter of the artery and the velocity of blood flow, but since the method presented in this article is a non-invasive method; both of these quantities should be measured non-invasively.

The best way to measure the blood velocity is using ultrasound and Doppler methods because ultrasonic waves are one of the least dangerous methods for measuring all kinds of vital quantities and the simplest imaging methods in the medical world. The procedure is carried out by

sending a wave having a particular frequency to the tissue or the target part of the body and depends on the quantity being measured either by discrete Doppler method or by continuous Doppler method, the measurements are implemented. According to clinical trials, the best frequency to measure blood flow through the artery is 4.63MHz, and the frequency of ultrasonic waves transmitted to measure vessel diameter is 5MHz because of having the highest rate of reflection by blood and arteries walls [73]. In relation 16, the parameters ρ and t are different for different individuals as the blood density and thickness of the vessel will change as the age goes up. Thus, to prove the validity of the presented relationship and also to show that the presented relationship has the least error, these two factors are identified as the causes of error in the measurement results and then the error caused by the effect of these two parameters on the measured pressure value was obtained. If we determine the amount of changes in blood density with $\Delta\rho$ and the changes in artery thickness with Δt , then we will have:

$$P = \frac{1}{\alpha} \ln \left(\frac{\rho d V^2}{t E_0} \right) = \frac{1}{\alpha} \ln \left(\frac{(\rho + \Delta\rho) d V^2}{(t + \Delta t) E_0} \right)$$

$$P = \frac{1}{\alpha} \ln \left(\frac{\rho \left(1 + \frac{\Delta\rho}{\rho} \right) d V^2}{t \left(1 + \frac{\Delta t}{t} \right) E_0} \right) = \frac{1}{\alpha} \ln \frac{\rho d V^2}{t E_0} \times \frac{1 + \frac{\Delta\rho}{\rho}}{1 + \frac{\Delta t}{t}} \tag{17}$$

$$P = \frac{1}{\alpha} \left[\ln \frac{\rho d V^2}{t E_0} + \ln \frac{1 + \frac{\Delta\rho}{\rho}}{1 + \frac{\Delta t}{t}} \right]$$

The second term in the above equation is equal to the error arisen from the density and the thickness so we will have:

$$error = \ln \left(\frac{1 + \frac{\Delta\rho}{\rho}}{1 + \frac{\Delta t}{t}} \right) = \ln \frac{1 + \frac{\Delta\rho}{\rho} + \frac{\Delta t}{t} - \frac{\Delta t}{t}}{1 + \frac{\Delta t}{t}} = \ln \left(1 + \frac{\frac{\Delta\rho}{\rho} - \frac{\Delta t}{t}}{1 + \frac{\Delta\rho}{\rho}} \right) \tag{18}$$

Concerning the Taylor expansion of the logarithmic function, we can write:

$$\ln(1 + u) = u - \frac{u^2}{2} + \frac{u^3}{3} - \dots$$

$$error = \frac{\frac{\Delta\rho}{\rho} - \frac{\Delta t}{t}}{1 + \frac{\Delta\rho}{\rho}} - \frac{\left(\frac{\frac{\Delta\rho}{\rho} - \frac{\Delta t}{t}}{1 + \frac{\Delta\rho}{\rho}} \right)^2}{2} + \frac{\left(\frac{\frac{\Delta\rho}{\rho} - \frac{\Delta t}{t}}{1 + \frac{\Delta\rho}{\rho}} \right)^3}{3} - \dots \tag{19}$$

If $\Delta\rho/\rho$ and $\Delta t/t$ have the same signs, then the numerators of the fractions are reduced and the error value is reduced. If $\Delta\rho/\rho$ and $\Delta t/t$ have opposite signs, then we will have the highest amount of error: There are two states for having opposite signs, in the first case when $\Delta\rho/\rho$ is positive and $\Delta t/t$ is negative, there will be:

$$error = \frac{\frac{\Delta\rho}{\rho} + \frac{\Delta t}{t}}{1 - \frac{\Delta t}{t}} \tag{20}$$

The numerator of the fraction will be positive and the denominator of the fraction will be less than one, and as the subsequent statements are subtracted, the error will be reduced.

In the second case, if $\Delta\rho/\rho$ is negative and $\Delta t/t$ is positive, we will have:

$$error = \frac{-\frac{\Delta\rho}{\rho} - \frac{\Delta t}{t}}{1 + \frac{\Delta t}{t}} \tag{21}$$

The numerator will be negative and the denominator of the fraction will be greater than one, so we will have the highest rate of error.

If $\Delta\rho/\rho$ and $\Delta t/t$ is considered to be equal, then we will have:

$$error = \frac{2\frac{\Delta t}{t}}{1 - \frac{\Delta t}{t}}$$

$$\frac{x}{1+x} = (x - x^2 + x^3 + \dots) = x(1 - x + x^2 + \dots) \tag{22}$$

$$error = \frac{-2\frac{\Delta t}{t}}{1 + \frac{\Delta t}{t}} = -2 \left[\left(\frac{\Delta t}{t}\right) - \left(\frac{\Delta t}{t}\right)^2 + \left(\frac{\Delta t}{t}\right)^3 + \dots \right] \cong error = 2\frac{\Delta t}{t}$$

5 The measurement of the blood flow velocity in the artery using Doppler theorem

The Doppler phenomenon was originally proposed for frequency variations of the sound source in classical physics. According to this effect, whenever the receiver of the audio source is moving relative to an audio transmitter, the receiver receives a frequency other than that sent one by the audio source. Taking into account the relativity theorem, there is no difference in the movement of the sound transmitter rela-

tive to the sound receiver or the sound receiver toward the sound transmitter. In this case, the received wavelength will be different from the transmitted one. In the Doppler theorem in the above relations, is C the velocity of sound moving in the desired environment, λ is the wavelength, and F is the ultrasonic wave frequency. Now if the generator source moves at the speed of V:

$$f = c/\lambda$$

$$\lambda' = \frac{c \pm v}{f} = \frac{c \pm v}{c/\lambda} = \frac{\lambda(c \pm v)}{c}$$

$$\lambda' = \frac{c}{f'} = \frac{c \pm v}{f} \tag{23}$$

$$f' = \frac{c}{(c \pm v)} f$$

$$f' = \frac{v}{(v \pm v_s)} f$$

In equation 23, F is the frequency of the sent signal towards the moving fluid, V is the velocity of the movement of the waves in the desired environment, VS is the velocity of passing fluid and is the received frequency belonging to the reflected signal from the moving fluid, which can be readily obtained by knowing the velocity of movement in the body and the frequency of the signals being transmitted and received. This is related to the condition that the transmitter and receiver are beside each other without having any angles relative to each other But in construction of two sensor side by side, one has the role of transmitter and the other one the role of the receiver, there will always be an angle with the blood flowing through the artery, and having this angle would give a better and more accurate measurement. Using the following equation, we also include this angle in our analyses to give a more accurate measurement so the relation about the Doppler theorem for measuring blood flow velocity can be rewritten as follows: [69-71]

$$V = \frac{c}{2 \cos \theta} \left(\frac{F_2 - F_1}{F_1} \right) \tag{24}$$

In equation 24, V is the velocity of the passing blood, F1 the frequency of the transmitted signal and F2 is the frequency of the received signal, and the difference between these two frequencies is known as Doppler shift. Also, in the equation above, θ is the angle between the ultrasonic signal transmitted and the blood flowing through the artery which will be adjusted once the device is constructed and it will be fixed, and C is the rate of movement of ultrasonic waves in body tissues.

The operation of the above system is shown in Figure 3, where the signal is transmitted from the transmitter sensor to the target vessel and it is reflected in the artery after moving through the blood. Then, the receiver sensor receives the reflected signal, and the Doppler shift can be obtained by detecting the frequency of the received signal. The accuracy of the system is very high because the only vessel near the elbow through which blood passes is the arterial vessel. It should be noted that there are other vessels at the location of measurement, but due to their small diameter or sub-arteries, they will have a smaller Doppler shift compared to the main vessel, and accordingly, to solve this problem, the receiver takes into account the highest difference of the received frequency. So, this problem is resolved automatically and what we have in the output is the velocity of the blood passing through the target artery.

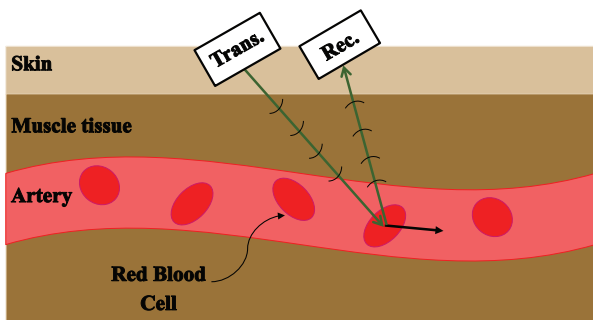
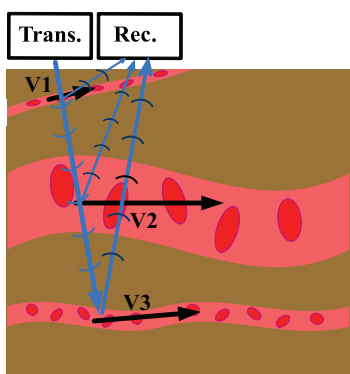


Figure 4: How to apply Doppler theorem to measure the blood velocity in an artery

How to select the desired vessel from the vessels at the site of measurement is based on the selection of the highest frequency difference. Since there are no other vessels near the target vessel, even if the sensor is not positioned in the proper location, it will still be possible to detect the passage of blood correctly because the vessel has the highest rate of passing through it, and the adjacent arteries are much slower than the main artery and have a very little impact on the transmitted frequency. Then, by performing a maximization step, it practically filters out the effect of the other veins and

the resulting change in the received frequency is due to the main artery and our target vessel, as shown in Figure 4. The method of measuring blood velocity will be as in the block diagram of Figure 5, in which the block diagram sends a number of ultrasonic sensors acting as a transmitter and transmits a sound having the frequency of 4.63MHz to the target artery. This frequency is generated by the generator signal block. Another ultrasonic sensor that plays the role of the receiver receives the frequency-shifted signal from the blood flow and sends it to the divider block after passing through an amplifier step. At the output of this block, we also have the frequency resulting from the division of the transmitted and the received signals. The output of the subtractor output is sent to the processor where along with the other required components, the desired process is performed and the blood flow rate is extracted.

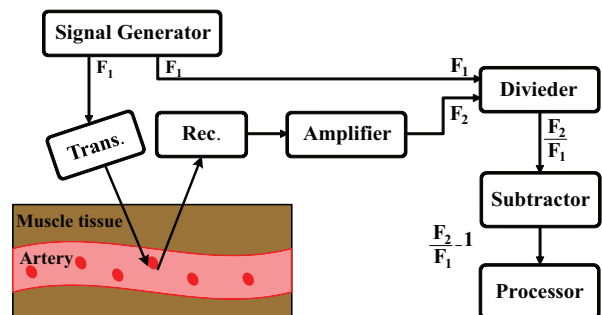


Figure 5: Block diagram of detection of the blood velocity

6 The measurement of vessel diameter using Doppler theorem

As mentioned before, applying the ultrasonic system and the Doppler theorem can be done in two ways of continuous Doppler discrete Doppler. The Doppler transmits the ultrasonic waves continuously and the other sensor receives the reflected signal, and by synthesizing the received signal and extracting its frequency, the desired measurement can be made. This method based upon Doppler theorem is very useful for velocity measurement, and in the medical world, and especially in sonographic devices, this technique is used to find the rate of blood flowing through different parts of the body, as well as to detect vascular congestion and even blood flow in the fetus.

An ultrasonic signal is sent to the desired location to measure the diameter of the artery, and with respect to the reflections made from different interior and exterior walls and so on the depth as well as the distance from the desired part to the sensor and body surface as well as the thickness can be measured and even it is feasible to

obtain a three-dimensional shape of the desired body by considering the differences between the reflections made from different parts. We used this technique in this article to measure the vessel diameter. The procedure is done in this way that using the signal with specific frequency after being transmitted by the transmitter sensor and the reflections made from the vessel walls; the diameter of the vessel can be detected. According to clinical trials, the vessel wall with the frequency of 5 MHz has the highest response and the highest reflection as well. In this case, the time difference between the signals with the highest amplitude (the arteries with thicker wall diameters have more reflection at the desired frequency and reflect the transmitted signal more) will be equal to the sweep time of the signal from the vessel walls and then through which the diameter of the vessel can be calculated. The schematic function of the measurement of the vessel diameter system is shown in Figure 6 and the block diagram of the vessel diameter detection system is shown in Figure 7. Since, however, the material the arterial wall is made of differs from that of the vein, and the frequency chosen to be transmitted toward the artery to measure artery diameter is proportional to the structure and material of the arteries, and most of the reflection is made from the arterial wall, not the vein, so, the selection of the arterial vessels will be done with a high accuracy.

According to Figure 7, the system functions in this way that the signal is transmitted by the transmitter sensor at a frequency of 5 MHz and after colliding with the outer wall of the vessel, some portion of the signal is reflected and the rest continues its way and colliding with the other wall of the vessel, it will be reflected. By having the time difference between the first reflected signal and the second reflected signal and the wave velocity in the body tissues using equation 25, we can obtain the desired artery diameter. Here, d is the diameter of the desired artery, C is the velocity of ultrasonic movement in the body and Δt is the time difference between the two signals reflected from the two vessel walls. The signals reflected through the vessel wall pass through an amplifier block and go into the Level Detector block. In this block, by detecting amplified signal edges, a counter is

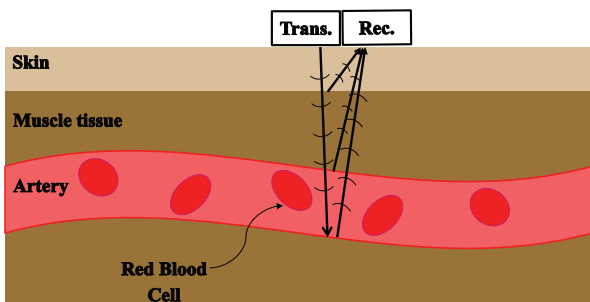


Figure 6: The mechanism of the measurement of artery diameter

applied and starts counting at a specified frequency that can be obtained by measuring the amounts counted to obtain the diameter of the vessel.

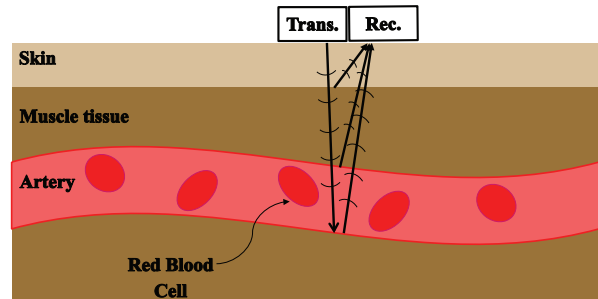


Figure 7: The block Diagram of the Measurement of artery Diameter

$$d = \frac{C \cdot \Delta t}{2} \tag{25}$$

7 The implementation of the total system of blood pressure measurement

The block diagram of the total system for measuring the BP will be in figure 8. In this figure, the solid lines are related to the control path and the continuous lines are belonging to the data path. According to the descriptions above, using the ultrasonic sensors of the receiver the desired signal after being received is amplified and loaded into the Frequency detector and Time Detector

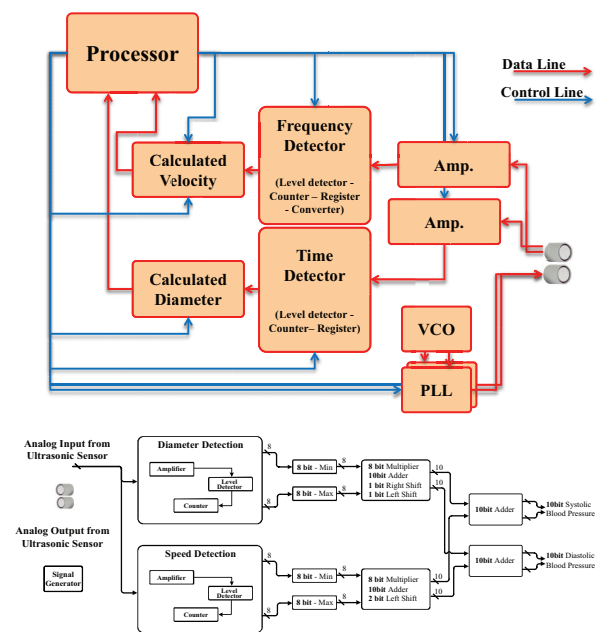


Figure 8: The block Diagram of the total BP measurement system

block and then, from these blocks the velocity and the diameter of the blood artery are extracted. Finally, in the Processor block, the necessary processes are performed according to equation 17 and the BP is obtained.

To demonstrate the correct performance of the proposed equations, we used MATLAB software; we considered the blood velocities in the range of 30-50 cm/s and the vessel diameter 1.6-3.4mm to be variables, assuming that the other parameters in the equation 18 were constant. Also, we considered the value of α as a constant coefficient of the vessel to be 0.017mmHg-1, E_0 Young’s modulus at zero pressure to have the constant value of 4.5kPa, ρ representing the blood density of 1080 kg/m³ and the approximate thickness of the vessels to be 0.46mm. [73] After simulating the above relationship, the ranges of high and low BP changes were obtained as 135mmHg and 73mmHg, respectively. The effect of instantaneous changes in the artery diameter and blood flow velocity that are inversely correlated is clearly shown in Figure 9.

In order to verify the correct operation of the proposed method and its equations, clinical testing was performed at Urmia Shams Cardiology Center (Iran). The test was performed simultaneously on one person in two ways; one using a Finapres BP monitor NOVA (Finapres Medical Systems, Enschede, Netherlands) and the other one using an ultrasonic sensor.

The NOVA device is able to measure the BP at the moment, so it records the person’s BP momentarily and simultaneously we can simultaneously obtain the vessel diameter using the ultrasonic sensor and blood

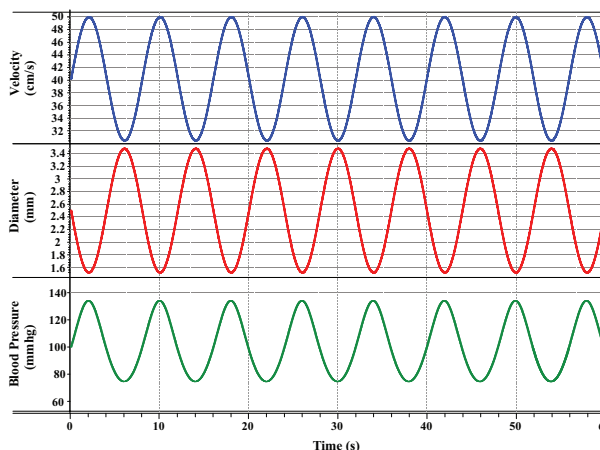


Figure 9: The simulation of BP due to changes in the velocity and diameter of the artery

velocity and later, applying the proposed method we obtained the person’s BP. We compared the results of the systolic and diastolic BP measurements and MAP for 60 seconds with the NOVA device and the proposed method, and the curves presented in Figure 10 show the results of these measurements.

The test was performed on the person in two different ways, one when the person was holding his or her breath and the other one when the person was breathing normally. In the curves in Figure 10, the dashed lines (blue) are the results obtained from the NOVA and the solid lines (red) are the results of the instantaneous measurement of BP by the proposed method. By examining the results of the two methods, one can clearly show the accuracy of the measurement using the presented system.

Table 1: The comparison of mean and standard deviation values measured by Sphygmomanometer desktop device using the proposed method

		MEAN(mmHg)	SD(mmHg)	Min (mmHg)	Max(mmHg)
Measure with RDMS device	DBP	65.16	10.31	51.3	112
	SBP	110.47	10.50	90.6	146
	MAP	80.3	10.18	65.1	122.2
Measure by proposed method	DBP	65.04	10.91	47.82	114.40
	SBP	110.24	11.28	90.63	148.49
	MAP	80.11	10.47	63.31	124.50

Table 2: The comparison of the results of the proposed method with the AAMI standard.

		MEAN(mmHg)	SD (mmHg)	Subject
Proposed Method Results	DBP	0.118	4.218	211
	MAP	0.015	3.235	211
	SBP	-0.233	4.538	211
AAMI[58]	BP	≤ 5	≤ 8	85 ≤

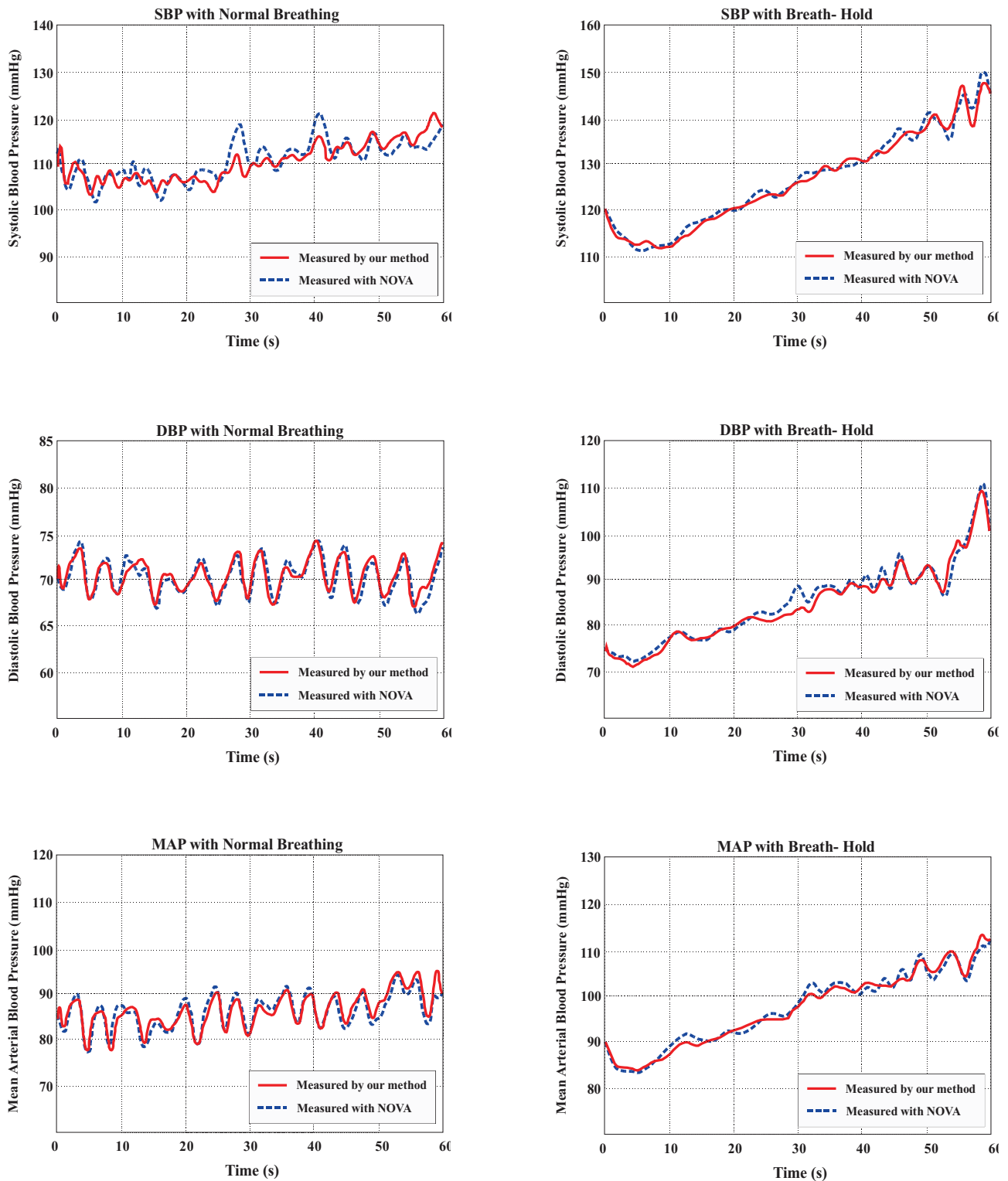


Figure 10: The results of a person’s BP test in two different ways

8 Database

The number of patients selected for measuring the BP was measured was 211, from whom 122 were males

and 89 were females. For each individual, Sampling was taken twice. Hence the number of samples was 422. This test was performed at various medical and clinical centers, and for all individuals, both systolic and diastolic BPs were measured using the Riester Dip-

Table 3: The comparison of the results of this paper with the BHS standard.

		Cumulative Error Percentage		
		≤ 5 mmHg	≤ 10 mmHg	≤ 15 mmHg
BHS Standard [59]	Grade A	60%	85%	95%
	Grade B	50%	75%	90%
	Grade C	40%	65%	85%
Proposed Method Results	SBP	164(78.09%)	197(93.8%)	207(98.6%)
	DBP	162(77.2%)	202(96.2%)	209(99.5%)
	MAP	191(90.6%)	209(99.5%)	210(100.%)

lomat Mercury Sphygmomanometer (RDMS) desktop monitor and the proposed method. The results of this review are presented in Table 1. The histogram diagram of this test with the desktop device is also shown in Figure 11. To demonstrate the correct performance of the proposed method, these results are compared with two of the most important and accepted standards in this field.

The validity of the proposed method was evaluated in the Association for the Advancement of Medical Instrumentation (AAMI) standard, based on ME (Mean Error) and SD (Standard Deviation). According to this standard, if the proposed method is experimented on at least 255 separate samples, the results will be reliable. This standard also allows a maximum of 3 samples per person, so at least 85 people must take the test. According to this standard, the validity of a method is confirmed when the measured ME is less than 5 mmHg and the SD is less than 8 mmHg. By comparing the values obtained from the measurements using the proposed method and the standard requirements of AAMI, it is revealed that all cases are acceptable and the values of SD and ME are lower than the expected values and the number of people tested is higher than the number of people required by the standard. In addition, the accuracy of the proposed method was also evaluated by the British Hypertension Society (BHS) standard. In this standard three different grades are reported based on the cumulative error percentage. From the samples at least 85 should be examined, which is similar to the AAMI standard. The acceptable error values according to the BHS standard [59] along with a comparison of the results obtained from the method presented under this standard are presented in Table 3. By comparing the results of BHS standard and proposed method in all grades the results have much better conditions than the standard requirements and they are true for all three SBP, DBP, and MAP cases. Therefore, the proposed method meets the requirements of both BHS and AAMI standards. Figure 12 presents the rates of the errors created between the measurements using the RDMS model mercury Sphygmomanometer desktop

and the proposed barometer. The graph shows that the error rates in the various measurements of SBP, DBP, and MAP have the highest correlation with the actual pressure value.

It should be noted that the database used in this work contains SBP and DBP pressure data measured by RDMS and Aixplorersonographic probe manufactured by Supersonic Imagine to measure blood velocity and diameter of patients in different wards of Shams hospitals in Urmia city. But the research data in [65] and [67] were collected from healthy people. The results of the proposed method will undoubtedly be improved if healthy people's data are added to the database. Better convergence results can be obtained provided that the number of samples in a database increases. According to the AAMI standard, one person's data can be used up to three times in the database, but in this study we used the data belonging to 211 persons and each person was sampled twice and with increasing it to three times the accuracy of the result can be amended unlike other studies, as in [12] and [66], that used fewer people with more sampling. In many studies, calibration has been used to improve results, but our proposed method does not require any calibration. Table 4 shows a comparison between the proposed method and the other methods. Figure 13 illustrates the measurement of vessel diameter and blood velocity using an ultrasound probe and these results were analyzed using MATLAB software. At the same time, we measured BP using a Sphygmomanometer desktop device. Both methods had similar results for systolic and diastolic BP.

9 Acknowledgments

Special thanks to the respected physicians of Shams Heart Hospital and Seyyed-al Shohada University Heart Hospital and Imam Khomeini Hospital in Urmia, including Dr. Rasoul Abbas Gholizadeh, Dr. EhsanMozafari, Dr. Mehdi MehdiZadeh, Dr. Kamal KhademVatan and Dr. Muhammedi as cardiologists, and Dr. Siah, Dr. Khashti and Dr. Sanei, as radiologists who have assisted in this research.

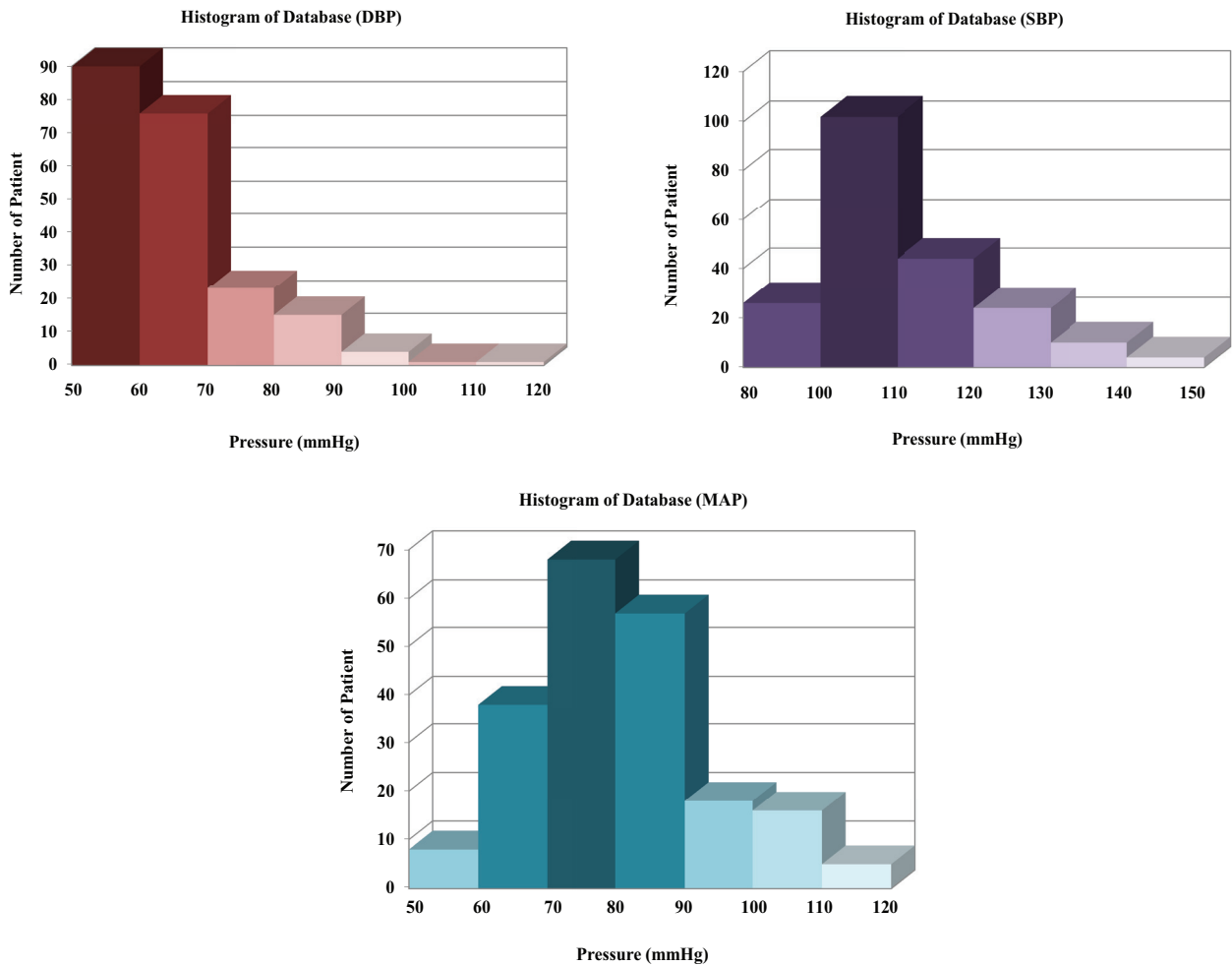


Figure 11: The Histogram diagram for the database presented in this article

Table 4: The comparison between the proposed method and the other methods.

Work	Subject	Record	DBP			SBP			MAP		
			ME	SD	RMSE*	ME	SD	RMSE*	ME	SD	RMSE*
[63]	32	7678	3.67	5.69	-	4.77	7.68	-	3.85	5.87	-
[61]	-	3000	0.03	4.72	-	0.16	6.85	-	-	-	-
[62]	69	69	0.01	4.66	-	0.06	7.08	-	-	-	-
[64]	113	113	7E-15	9.45	-	-1.9E-16	13.81	-	9.3E-7	10.44	-
[14]	-	910	-	-	5.8	-	-	10.9	-	-	-
[65]	10	-	-	-	-	3.8	4.2	-	-	-	-
[12]	19	7000	-	-	-	-	-	-	-	-	-
[33]	-	250	1.92	2.47	-	2.32	2.91	-	-	-	-
[60]	-	15000	-	-	-	-	-	-	-	-	-
[66]	32	7000	-	-	-	-	-	-	-	-	-
[67]	65	78	4.6	4.3	-	5.1	4.3	-	-	-	-
[68]	572	53708	-3.65	8.69	-	-2.98	19.35	-	-3.38	10.35	-
This	211	422	0.118	4.218	4.20	-0.233	4.538	4.53	0.015	3.235	3.22

* Root Mean Square Error.

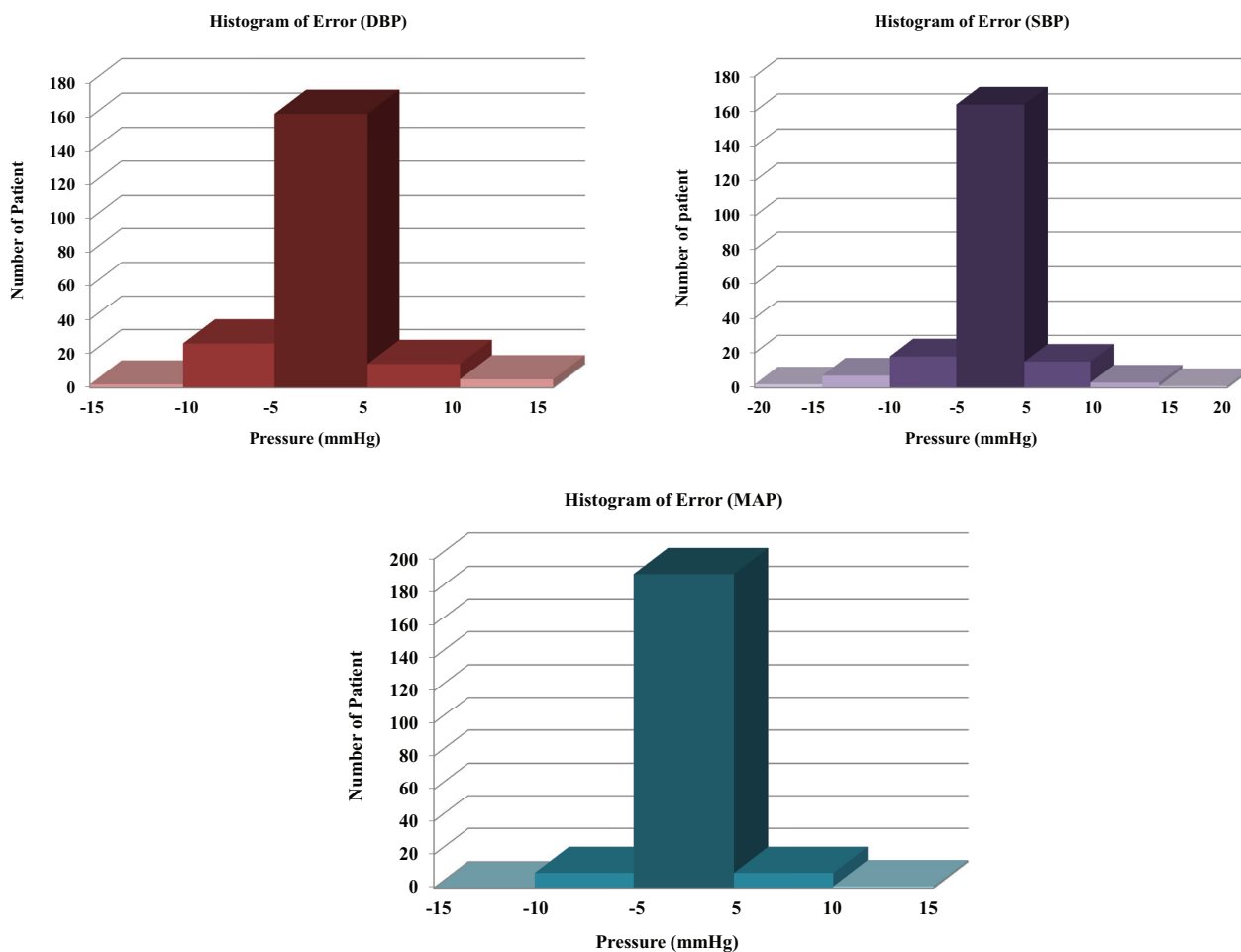


Figure 12: The histogram of the measured error based on the proposed method compared to the RDMS desktop device

10 Conclusions

In this paper, a new method based on the use of ultrasonic signals for BP measurement is presented, which is a non-invasive and continuous method and does not require calibration. In this study, the problems of previous methods such as different PTT-based measurements with PPG and ECG sensors or BP estimation methods that only estimate BP by measuring one quantity of vessels have been resolved. The proposed method was measured by calculating the diameter of the artery and the velocity of the blood passing through using ultrasonic waves, and then we obtained the BP using the presented equations. Finally, the comparative results show that the proposed algorithm is better than previous methods for accurate measurement of BP considering the results obtained for all three parameters of DBP, SBP, and MAP. This method fully meets the requirements for AAMI and BHS standards, which are valid in this field.

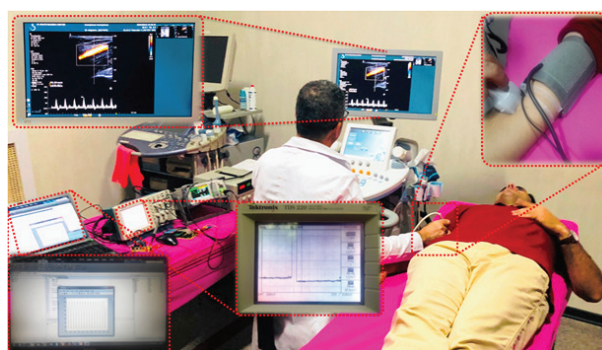


Figure 13: Measurement of vessel diameter and blood velocity instantaneously using Aixplorer ultrasound, the proposed method, and RDMS

11 Conflict of Interest

The authors declare that there is no conflict of interest for this paper. Also, there are no funding supports for this manuscript.

12 References

1. M. Nichols, N. Townsend, P. Scarborough, M. Rayner, Cardiovascular disease in Europe: epidemiological update, *Eur. Heart J.* 34 (2013) 3028–3034.
<https://doi.org/10.1093/eurheartj/ehu299>
2. W. H. Organization, et al., World Health Statistic 2015, World Health Organization, 2015.
3. V. Perkovic, R. Huxley, Y. Wu, D. Prabhakaran, S. MacMahon, The burden of blood pressure-related disease: a neglected priority for global health, *Hypertension* 50 (2007) 991–997.
<https://doi.org/10.1161/HYPERTENSIONAHA.107.095497>
4. X.-R. Ding, N. Zhao, G.-Z. Yang, R.I. Pettigrew, B. Lo, F. Miao, et al., Continuous blood pressure measurement from invasive to unobtrusive: celebration of 200th birth anniversary of Carl Ludwig, *IEEE J. Biomed. Health Inform.* 20(2016) 1455–1465.
<https://doi.org/10.1109/JBHI.2016.2620995>
5. L. Peter, N. Noury, M. Cerny, A review of methods for non-invasive and continuous blood pressure monitoring: pulse transit time method is promising? *IRBM* 35 (2014) 271–282.
<https://doi.org/10.1016/j.irbm.2014.07.002>
6. P.A. Iazzo, *Handbook of Cardiac Anatomy, Physiology, and Devices*, Springer Science & Business Media, 2009.
7. N.H. Lung, B. Institute, *Diseases and Conditions Index: Hypotension*, 2008.
8. D. Buxi, J.-M. Redouté, M.R. Yuce, A survey on signals and systems in ambulatory blood pressure monitoring using pulse transit time, *Physiol. Meas.* 36 (2015), p. R1.
9. Y. Zheng, C.C. Poon, B.P. Yan, J.Y. Lau, Pulse arrival time based cuff-less and 24-H wearable blood pressure monitoring and its diagnostic value in hypertension, *J. Med. Syst.* 40 (2016) 195.
<https://doi.org/10.1007/s1091>
10. S. Mottaghi, M. Moradi, L. Roohisefat, Cuffless blood pressure estimation during exercise stress test, *Int. J. Biosci. Biochem. Bioinform.* 2 (2012) 394.
11. L. Geddes, M. Voelz, C. Babbs, J. Bourland, W. Tacker, Pulse transit time as an indicator of arterial blood pressure, *Psychophysiology* 18 (1981) 71–74.
<https://doi.org/10.1111/j.1469-8986.1981.tb01545.x>
12. Y. Zhang, Z. Feng, A SVM method for continuous blood pressure estimation from a PPG signal, in: *Proceedings of the 9th International Conference on Machine Learning and Computing*, 2017, pp. 128–132.
<https://doi.org/10.1145/3055635.3056634>
13. C. Sideris, H. Kalantarian, E. Nematy, M. Sarrafzadeh, Building continuous arterial blood pressure prediction models using recurrent networks, in: *2016 IEEE International Conference on Smart Computing (SMARTCOMP)*, 2016, pp. 1–5.
<https://doi.org/10.1109/SMARTCOMP.2016.7501681>
14. M. Liu, P. Lai-Man, H. Fu, Cuffless blood pressure estimation based on photoplethysmography signal and its second derivative, *Int. J. Comput. Theory Eng.* 9 (2017) 202.
<https://doi.org/10.7763/IJCTE.2017.V9.1138>
15. Mendis, Shanthi; Puska, Pekka; Norrving, Bo (2011). *Global atlas on cardiovascular disease prevention and control* (PDF) (1st ed.). Geneva: World Health Organization in collaboration with the World Heart Federation and the World Stroke Organization. p. 38. ISBN 9789241564373. Archived (PDF) from the original on 17 August 2014.
16. Jump up to: a b Hernandorena, I; Duron, E; Vidal, JS; Hanon, O (July 2017). "Treatment options and considerations for hypertensive patients to prevent dementia". *Expert Opinion on Pharmacotherapy* (Review). 18 (10): 989–1000.
<https://doi.org/10.1080/14656566.2017.1333599>. PMID 28532183.
17. Lau, DH; Nattel, S; Kalman, JM; Sanders, P (August 2017). "Modifiable Risk Factors and Atrial Fibrillation". *Circulation* (Review). 136 (6): 583–96.
<https://doi.org/10.1161/CIRCULATIONAHA.116.023163>. PMID 28784826.
18. Parati G, Ochoa JE, Lombardi C, Salvi P, Bilo G, "Assessment and interpretation of blood pressure variability in a clinical setting," *Blood press*, vol. 22, no. 6, pp. 345-354, 2013.
<https://doi.org/10.3109/08037051.2013.782944>
19. Campbell NR, Chockalingam A, Fodor JG, McKay DW, "Accurate, reproducible measurement of blood pressure," *CMAJ* (Canadian Medical Association Journal), vol. 143, no. 1, pp. 19-24, 1990.
20. R. A. Payne, C. N. Symeonides, D. J. Webb, and S. R. J. Maxwell, "Pulse transit time measured from the ECG: an unreliable marker of beat-to-beat blood pressure," *J. Appl. Physiol.*, vol. 100, no. 1, pp. 136-141, 2006.
<https://doi.org/10.1152/jappphysiol.00657.2005>
21. E.C. Chua, S.J. Redmond, G. McDarby and C. Heneghan, "Towards using photoplethysmogram amplitude to measure blood pressure during sleep," *Annals of Biomedical Engineering*, vol. 38, no. 3, pp. 945-954, 2010.
<https://doi.org/10.1007/s10439-009-9882-z>
22. X. Xing and M. Sun, "Optical blood pressure estimation with photoplethysmography and FFT-based neural networks," *BIOMEDICAL OPTICS EXPRESS*, vol. 7, no. 8, pp. 3007-3020, 2016.
<https://doi.org/10.1364/BOE.7.003007>
23. Longmore, Sally K., Gough Y. Lui, Ganesh Naik, Paul P. Breen, Bin Jalaludin, and Gaetano D. Gargiulo. "A comparison of reflective photoplethysmography for detection of heart rate, blood oxy-

- gen saturation, and respiration rate at various anatomical locations." *Sensors* 19, no. 8 (2019): <https://doi.org/10.3390/s19081874>
24. W. Tao, T. Liu, R. Zheng and H. Feng, "Gait analysis using wearable sensors". *Sensors (Basel)*, vol. 4, pp. 2255–83, 2012. <https://doi.org/10.3390/s120202255>
 25. O. Olguin, P. Gloor, & A. Pentland, "Wearable Sensors for Pervasive Healthcare Management." *Principles and applications,* Proceedings of the IEEE, vol. 66, pp. 1–4, 2009. <https://doi.org/10.4108/ICST.PERVASIVEHEALTH2009.6033>
 26. G. Appelboom, E. Camacho, M. E. Abraham, S. S. Bruce, E. L. P. Dumont, B. E. Zacharia, R. D'Amico, J. Slomian, J. Y. Redinster, O. Bruyère and E. S. Colony "Smart wearable body sensors for patient self-assessment and monitoring." *Arch. Public Health*, 72, p. 28, 2014. <https://doi.org/10.1186/2049-3258-72-28>
 27. N. Luo, J. Ding, N. Zhao, B. H. K. Leung & C. C. Y. Poon, "Mobile health: Design of flexible and stretchable electrophysiological sensors for wearable healthcare systems." 11th International Conference on Wearable and Implantable Body Sensor Networks, BSN 2014, pp. 87–91. <https://doi.org/10.1109/BSN.2014.25>
 28. S. Yao, & Y. Zhu, "Wearable multifunctional sensors using printed stretchable conductors made of silver nanowires." *Nanoscale*, vol. 6, p. 2345, 2014. <https://doi.org/10.1039/C3NR05496A>
 29. D. Vilela, A. Romeo & S. Sánchez, "Flexible sensors for biomedical technology." *Lab Chip* (2016). <https://doi.org/10.1039/C5LC90136G>
 30. Z. Zhang, Z. Pi, B. Liu, TROIKA: a general framework for heart rate monitoring using wrist-type photoplethysmographic signals during intensive physical exercise, *IEEE Trans. Biomed. Eng.* 62 (2015) 522–531. <https://doi.org/10.1109/TBME.2014.2359372>
 31. S.C. Millasseau, F.G. Guigui, R.P. Kelly, K. Prasad, J.R. Cockcroft, J.M. Ritter, et al., Noninvasive assessment of the digital volume pulse: comparison with the peripheral pressure pulse, *Hypertension* 36 (2000) 952–956.
 32. M. Kachuee, M.M. Kiani, H. Mohammadzade, M. Shabany, Cuffless blood pressure estimation algorithms for continuous health-care monitoring, *IEEE Trans. Biomed. Eng.* 64 (2017) 859–869. <https://doi.org/10.1109/TBME.2016.2580904>
 33. P. Li, M. Liu, X. Zhang, X. Hu, B. Pang, Z. Yao, et al., Novel wavelet neural network algorithm for continuous and noninvasive dynamic estimation of blood pressure from photoplethysmography, *Sci. China Inf. Sci.* 59 (2016), p.042405. <https://doi.org/10.1007/s11432-015-5400-0>
 34. Peterson LH, Jensen RE, Parnell J. Mechanical properties of arteries in vivo. *Circ Res.* 1960;8:622–639. <https://doi.org/10.1161/01.RES.8.3.622>
 35. Gosling RG. Extraction of physiological information from spectra analysed Doppler-shifted continuous wave ultrasound signals. *Peter Peregrinus UK IEE Med Electron Monographs.* 1976;21:73–125.
 36. O'Rourke MF, Staessen JA, Vlachopoulos C, Duprez D, Plante GE. Clinical applications of arterial stiffness: definitions and reference values. *Am J Hypertens.* 2002; 15:426–444. [https://doi.org/10.1016/S0895-7061\(01\)02319-6](https://doi.org/10.1016/S0895-7061(01)02319-6)
 37. *Handbook of Chemistry and Physics.* 76th ed. Boca Raton, Fla: Chemical Rubber Co; 1995–1996; section 6:137.
 38. *Chambers Dictionary.* London: Chambers Harrap Ltd; 1993:353.
 39. Frank O. Die Theorie de Pulswellen. *Ztschr Biol.* 1926;85:91–130.
 40. Bergel DH. The static elastic properties of the arterial wall. *J Physiol.* 1961;156:445–469. <https://doi.org/10.1113/jphysiol.1961.sp006686>
 41. Moens AI. Die Pulskurve. Leiden, Netherlands. 1878.
 42. Korteweg DJ. Uber die Fortpflanzungsgeschwindigkeit des Schalles in Elastiischen Rohren. *Ann Phys Chem (NS).* 1878;5:52–537. <https://doi.org/10.1002/andp.18782411206>
 43. Clark JM, Glagov S. Transmural organization of the arterial media: the lamellar unit revisited. *Arteriosclerosis.* 1985;5:19–34. <https://doi.org/10.1161/01.ATV.5.1.19>
 44. Roach MR, Burton AC. The reason for the shape of the distensibility curves of arteries. *Can J Biochem Physiol.* 1957;35:681–690. <https://doi.org/10.1139/o57-080>
 45. Bank AJ, Wang H, Holte JE, Mullen K, Shammas R, Kubo SH. Contribution of collagen, elastin, and smooth muscle to in vivo human brachial artery wall stress and elastic modulus. *Circulation.* 1996;94:3263–3270. <https://doi.org/10.1161/01.CIR.94.12.3263>
 46. Farrar DJ, Green HD, Bond MG, Wagner WD, Gobbie RA. Aortic pulse wave velocity, elasticity, and composition in a nonhuman primate model of atherosclerosis. *Circ Res.* 1978;43:52–62. <https://doi.org/10.1161/01.RES.43.1.52>
 47. Berry CL, Greenwald SE. Effects of hypertension on the static mechanical properties and chemical composition of the rat aorta. *Cardiovasc Res.* 1976;10:437–451. <https://doi.org/10.1093/cvr/10.4.437>
 48. Bergel DH. Arterial Viscoelasticity in Pulsatile Blood Flow. Attinger EO, ed. London: McGraw-Hill; 1964:279–290.

49. O'Rourke MF, Taylor MG. Input impedance of the systemic circulation. *Circ Res.* 1967;20:365–380. <https://doi.org/10.1161/01.RES.20.4.365>
50. Hayashi K, Sato M, Hauda H, Moritake K. Biomechanical study of the constitutive laws of vascular walls. *Exp Mech.* 1974;14:440–444. <https://doi.org/10.1007/BF02324024>
51. Hayashi K, Hauda H, Nagasawa S, Okuwura A, Moritake K. Stiffness and elastic behaviour of human intracranial and extracranial arteries. *J Biomech.* 1980;13:175–184. [https://doi.org/10.1016/0021-9290\(80\)90191-8](https://doi.org/10.1016/0021-9290(80)90191-8)
52. Kawasaki T, Sasayama S, Yagi S, Asakawa T, Hirai T. Non-invasive assessment of age-related changes in stiffness of major branches of the human arteries. *Cardiovasc Res.* 1987;21:678–687. <https://doi.org/10.1093/cvr/21.9.678>
53. Lehman ED, Gosling RG, Parker JR, de Silva T, Taylor MG. A blood pressure independent index of aortic distensibility. *Br J Radiol.* 1993;66: 126–131. <https://doi.org/10.1259/0007-1285-66-782-126>
54. Lehmann ED, Hopkins KD, Parker JR, Turay RC, Rymer J, Fogelman I, Gosling RG. Aortic distensibility in post-menopausal women receiving Tibolone. *Br J Radiol.* 1994;67:701–705. <https://doi.org/10.1259/0007-1285-67-799-701>
55. Lehmann ED, Hopkins KD, Jones RL, Rudd AG, Gosling RG. Aortic distensibility in patients with cerebrovascular disease. *Clin Sci (Lond).* 1995;89:247–253.
56. Van Bortel LM, Balkestein EJ, van der Heijden-Spek JJ, Vanmolkot FH, Staessen JA, Kragten JA, Vredeveld JW, Safar ME, Struijker Boudier HA, Hoeks AP. Non-invasive assessment of local arterial pulse pressure: comparison of applanation tonometry and echo-tracking. *J Hypertens.* 2001;19:1037–1044.
57. Laogun AA, Gosling RG. In vivo arterial compliance in man. *Clin Phys Physiol Meas.* 1982;3:201–212.
58. A. f. t. A. o. M. Instrumentation, American National Standard. Manual, Electronic or Automated Sphygmomanometers, ANSI/AAMI SP10-2002/A1, 2003.
59. E. O'Brien, B. Waeber, G. Parati, J. Staessen, M.G. Myers, Blood pressure measuring devices: recommendations of the European Society of Hypertension, *BMJ: Br. Med. J.* 322 (2001) 531. <https://doi.org/10.1136/bmj.322.7285.531>
60. Y. Kurylyak, F. Lamonaca, D. Grimaldi, A neural network-based method for continuous blood pressure estimation from a PPG signal, in: 2013 IEEE International Instrumentation and Measurement Technology Conference (I2MTC), 2013, pp. 280–283. <https://doi.org/10.1109/I2MTC.2013.6555424>
61. A. Gaurav, M. Maheedhar, V.N. Tiwari, R. Narayanan, Cuff-less PPG based continuous blood pressure monitoring—A smartphone based approach, in: IEEE 38th Annual International Conference of the Engineering in Medicine and Biology Society (EMBC), 2016, pp. 607–610. <https://doi.org/10.1109/EMBC.2016.7590775>
62. X. Xing, M. Sun, Optical blood pressure estimation with photoplethysmography and FFT-based neural networks, *Biomed. Opt. Express* 7 (2016) 3007–3020. <https://doi.org/10.1364/BOE.7.003007>
63. K. Duan, Z. Qian, M. Atef, G. Wang, A feature exploration methodology for learning based cuffless blood pressure measurement using photoplethysmography, in: IEEE 38th Annual International Conference of the Engineering in Medicine and Biology Society (EMBC), 2016, 2016, pp. 6385–6388. <https://doi.org/10.1109/EMBC.2016.7592189>
64. H. Jiang, F. Miao, M. Gao, X. Hong, Q. He, H. Ma, et al., A novel indicator for cuff-less blood pressure estimation based on photoplethysmography, in: International Conference on Health Information Science, 2016, pp. 119–128. https://doi.org/10.1007/978-3-319-48335-1_13
65. R. Gircys, A. Liutkevicius, A. Vrubliauskas, E. Kazanavicius, Blood pressure estimation according to photoplethysmographic signal steepness, *Inf. Technol. Control.* 44 (2015) 443–450. <https://doi.org/https://doi.org/10.5755/j01.itc.44.4.12562>
66. A.D. Choudhury, R. Banerjee, A. Sinha, S. Kundu, Estimating blood pressure using Windkessel model on photoplethysmogram, in: 2014 36th Annual International Conference of the IEEE Engineering in Medicine and Biology Society (EMBC), 2014, pp. 4567–4570. <https://doi.org/10.1109/EMBC.2014.6944640>
67. S.C. Gao, P. Wittek, L. Zhao, W.J. Jiang, Data-driven estimation of blood pressure using photoplethysmographic signals, in: 2016 IEEE 38th Annual International Conference of the Engineering in Medicine and Biology Society (EMBC), 2016, pp. 766–769. <https://doi.org/10.1109/EMBC.2016.7590814>
68. J.C. Ruiz-Rodríguez, A. Ruiz-Sanmartín, V. Ribas, J. Caballero, A. García-Roche, J. Riera, et al., Innovative continuous non-invasive cuffless blood pressure monitoring based on photoplethysmography technology, *Intensive Care Med.* 39 (2013) 1618–1625. <https://doi.org/10.1007/s00134-013-2964-2>
69. Spicer D.W. and Boyes W. Consumer guide to ultrasonic and correlation flowmeter. Copperhill and Pointer Inc. USA P.9. 2004.)
70. C. Carlander. installation Effect and Self Diagnostics for Ultrasonic Flow Measurement, Doctoral Thesis 2001:11. Department of computer and

- electrical engineering, Lulea University of Technology, 2004. ISSN 1402-1544.
71. James W. Bowen, Fundamentals of Ultrasonic Flow Meters, Instromet, Incorporated.
 72. Developing a Method of Measuring Blood Pressure Using a Video Recording Julia Jansson julia.jansson@gmail.com under the direction of Prof. Hamed Hamid Muhammed Department of Technology and Health Royal Institute of Technology Research Academy for Young.
 73. Seo, Joohyun, Sabino J. Pietrangelo, Hae-Seung Lee, and Charles G. Sodini. "Noninvasive arterial blood pressure waveform monitoring using two-element ultrasound system." IEEE transactions on ultrasonics, ferroelectrics, and frequency control 62, no. 4 (2015): 776-784.
<https://doi.org/10.1109/TUFFC.2014.006904>
 74. Kowalewski, Tomasz A. "Blood Flow-Modelling and Diagnostics: Advanced Course and Workshop-BF 2005, Warsaw, June 20-23, 2005." Lecture Notes-ABIOMED (2005).
 75. Athanasiou, Kyriacos A., and Roman M. Natoli. "Introduction to continuum biomechanics." Synthesis lectures on biomedical engineering 3, no. 1 (2008): 1-206.
<https://doi.org/10.2200/S00121ED1V01Y200805BME019>
 76. McNaught, Alan D. Compendium of chemical terminology. Vol. 1669. Oxford: Blackwell Science, 1997.
 77. Truesdell, Clifford, and Leonhard Euler. The Rational Mechanics of Flexible Or Elastic Bodies, 1638-1788: Introduction to LeonhardiEuleri Opera Omnia Vol X Et XI SerieiSecundae. Vol. 11.OrellFüssli, 1960.
 78. Manning, Warren J., and Dudley J. Pennell. Cardiovascular Magnetic Resonance: A Companion to Braunwald's Heart Disease E-Book. Elsevier Health Sciences, 2018.
 79. Wiedeman, Mary Purcell. An introduction to microcirculation. Vol. 2. Elsevier, 2012.
 80. Button, Vera. Principles of Measurement and transduction of biomedical variables. Academic Press, 2015.



Copyright © 2020 by the Authors.
This is an open access article distributed under the Creative Commons

Attribution (CC BY) License (<https://creativecommons.org/licenses/by/4.0/>), which permits unrestricted use, distribution, and reproduction in any medium, provided the original work is properly cited.

Arrived: 31. 12. 2019

Accepted: 14. 05. 2020